



Clouds damp the impacts of Polar sea ice loss

1
2
3

4 **Authors:** Ramdane Alkama^{1*}, Alessandro Cescatti¹, Patrick C. Taylor², Lorea Garcia-San
5 Martin¹, Herve Douville³, Gregory Duveiller¹, Giovanni Forzieri¹ and Didier Swingedouw⁴

6

7 **Affiliation:**

8 ¹ European Commission, Joint Research Centre, Via E. Fermi, 2749, I-21027 Ispra (VA), Italy

9 ² NASA Langley Research Center, Hampton, Virginia

10 ³ Centre National de Recherches Meteorologiques, Meteo-France/CNRS, Toulouse, France

11 ⁴ EPOC, Universite Bordeaux 1, Allée Geoffroy Saint-Hilaire, Pessac 33615, France

12

13 ***Correspondence to:** Ramdane Alkama (ram.alkama@hotmail.fr)

14

15 **Abstract**

16 Clouds play an important role in the climate system through two main contrasting effects: (1)
17 cooling the Earth by reflecting part of incoming solar radiation to space; (2) warming the Earth by
18 reducing the loss of thermal energy to space. Recently, a significant amount of attention has been
19 given to the influence of clouds on the Arctic surface energy budget. Studies have argued that
20 clouds cover fraction is not responding to reduced sea ice in summer. Taking a different perspective
21 in this work using CERES data and 32 CMIP5 climate models, we find that the shortwave cooling
22 effect of clouds strongly influences the surface energy budget response to changes in sea ice cover.
23 The results illustrate that the cloud cooling effect operates in a counter-intuitive manner of the
24 polar seas: years with less sea ice and a larger net surface radiative flux are also those that show
25 an increase in sunlight reflected back to space by clouds. An increase in absorbed solar radiation
26 when sea ice retreats (surface albedo change) explains $66 \pm 2\%$ of the observed signal. The
27 remaining $34 \pm 1\%$ are due to the increase in cloud cover/thickness. This interplay between clouds
28 and sea ice reduces by half the increase of net radiation at the surface that follows the sea-ice
29 retreat, therefore damping the surface energy budget impact of polar sea ice loss. We further
30 highlight how this process is represented in some climate models.

31
32
33
34
35
36



37 **1. Introduction**

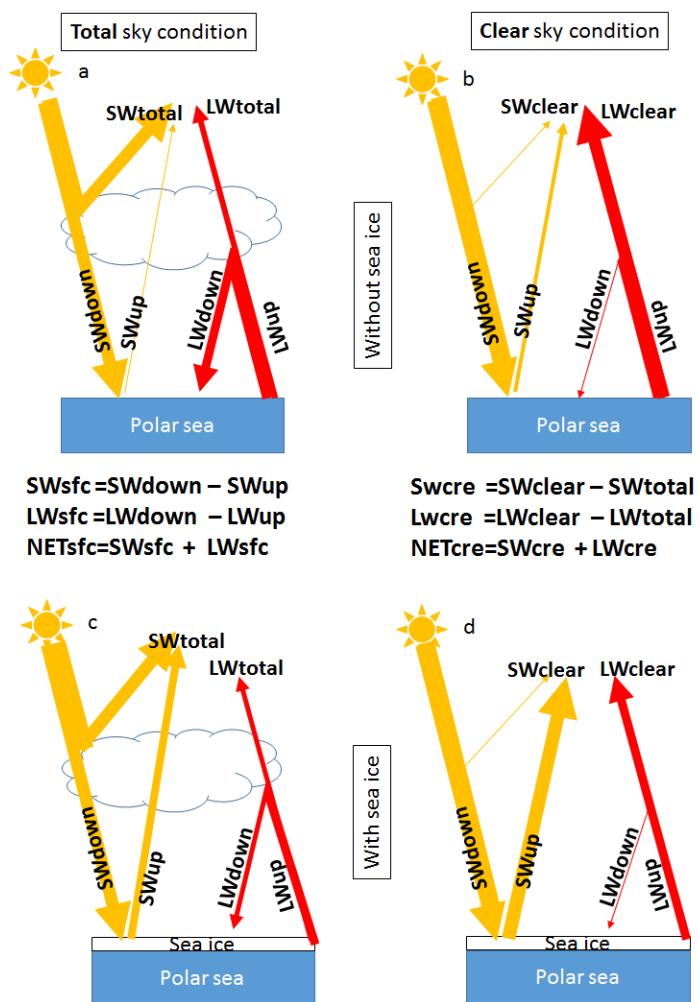
38 Radiation from the sun is the primary energy source to the Earth system and is responsible for the
39 energy driving motions in the atmosphere and ocean, for the energy behind water phase changes,
40 and for the energy stored in fossil fuels. Only a fraction (Loeb et al., 2018) of the solar energy
41 arriving to the top of the Earth atmosphere (shortwave radiation, SW) is absorbed at the surface.
42 Some of it is reflected back to space by clouds and by the surface, while some is absorbed by the
43 atmosphere. In parallel, the Earth's surface and atmosphere emit thermal energy back to space,
44 called outgoing longwave (LW) radiation, resulting in a loss of energy (Fig. 1). The balance
45 between these energy exchanges determine Earth's present and future climate. The change in this
46 balance is particularly important over the Arctic where summer sea ice is retreating at an
47 accelerated rate (Comiso et al., 2008), surface albedo is rapidly declining, and surface temperatures
48 are rising at a rate double that of the global average (Cohen et al., 2014; Graversen et al., 2008),
49 impacting sub-polar ecosystems (Cheung et al., 2009; Post et al., 2013) and possibly mid-latitude
50 climate (Cohen et al., 2014).

51 Clouds play an important role in modifying the radiative energy flows that determine Earth's
52 climate. This is done both by increasing the amount of SW reflected back to space and by reducing
53 the LW energy loss to space relative to clear skies (Fig 1). These cloud effects on Earth's radiation
54 budget can be gauged using the Cloud Radiative Effect (CRE), defined as the difference between
55 the actual atmosphere and the same atmosphere minus the clouds (Charlock and Ramanathan,
56 1985). The different spectral components of this effect can be estimated from satellite
57 observations: the global average shortwave (SW) cloud radiative effect (SWcre) is negative since
58 clouds reflect incoming solar radiation back to space resulting in a cooling effect. Alternatively,
59 the longwave cloud radiative effect (LWcre) is positive since clouds reduce the outgoing LW
60 radiation to space generating a warming effect (Harrison et al., 1990; Loeb et al., 2018;
61 Ramanathan et al., 1989).

62 In this study, we use the Clouds and the Earth's Radiant Energy System (CERES) top-of-
63 atmosphere (TOA) radiative flux dataset and 32 CMIP5 climate models to estimate the relationship
64 between the CRE and the Earth's surface radiation budget.

65

66



67

68 **Figure 1** Schematic representation of radiative energy flows in polar seas under total sky
 69 conditions (a, c) and clear sky conditions (b, d) for two contrasting surface conditions: without sea
 70 ice (a, b) and with sea ice (c, d).

71

72 2. Methods and data

73 **2.1 Cloud Radiative Effect:** CRE is used as a metric to assess the radiative impact of clouds on
 74 the climate system, defined as the difference in net irradiance at TOA between total-sky and clear-
 75 sky conditions. Using the CERES EBAF Ed4.0 (Loeb et al., 2018) flux measurements and CMIP5
 76 modeled flux, CRE is calculated by taking the difference between clear-sky and total-sky net
 77 irradiance flux at the TOA.

78 $SW_{cre} = SW_{total} - SW_{clear}$ (1)



79 $LW_{cre}=LW_{total} - LW_{clear}$ (2)

80 $NET_{cre}=SW_{cre} + LW_{cre}$ (3)

81

82 **2.2 Earth's surface radiative budget:** The net SW and LW flux at the surface (SW_{sfc} and LW_{sfc} ,
83 respectively) is calculated as the difference between incoming SW_{down} (LW_{down}) and outgoing
84 SW_{up} (LW_{up}) as shown in equations 4 (5).

85 $SW_{sfc}=SW_{down}- SW_{up}$ (4)

86 $LW_{sfc}=LW_{down} - LW_{up}$ (5)

87 $NET_{sfc}=SW_{sfc} + LW_{sfc}$ (6)

88

89 **2.3 CERES EBAF Ed4.0 Products:** For all surface and TOA radiative flux quantities, we used
90 the NASA CERES Energy Balanced and Filled (EBAF) monthly data set (CERES EBAF-
91 TOA_Ed4.0), providing monthly, global fluxes on a 1-degree latitude by 1-degree longitude grid.

92 The CERES EBAF product is a standard source for estimating surface irradiance at the global
93 scale (Loeb et al., 2018). In this study, we used CERES surface longwave (LW) and shortwave
94 (SW) radiative fluxes to investigate the influence of clouds on the variability in the Arctic surface
95 energy budget in conjunction with variations in sea ice. CERES EBAF-TOA-Surface products
96 have demonstrated improved the accuracy of TOA-surface irradiance computations relative to
97 other sources (e.g., meteorological reanalysis), and the errors/uncertainties between observed
98 monthly mean irradiances and EBAF-TOA-Surface fluxes are small (Kato et al., 2013).

99 **2.4 Sea ice concentration:** Sea ice concentration (SIC) data are from the National Snow and Ice
100 Data Center (NSIDC, <http://nsidc.org/data/G02202>). This data set provides a Climate Data Record
101 (CDR) of SIC from passive microwave data. It provides a consistent, daily and monthly time series
102 of SIC from 09 July 1987 through the most recent processing for both the North and South Polar
103 regions (Peng et al., 2013; W. Meier, F. Fetterer, M. Savoie, S. Mallory, R. Duerr, 2017). The data
104 is on a 25 km x 25 km grid. We used the latest version (Version 3) of the SIC CDR created with a
105 new version of the input product, from Nimbus-7 SMMR and DMSP SSM/I-SSMIS Passive
106 Microwave Data.

107 **2.5 Polar seas:** We defined polar seas as the seas where we observed monthly SIC larger than 10%
108 at least one month during 2001-2016 period. Polar seas extent is shown in Figure S1.

109 **2.6 CMIP5 Models** To reconstruct the historical CRE and surface energy budget and project their
110 future changes, we used an ensemble of simulations conducted with 32 earth system models
111 (models used are shown in Figure 3 and S3) contributing to the Coupled Model Intercomparison



112 Project Phase 5 (CMIP5) (Taylor et al., 2012). These model experiments provided: historical runs
113 (1850-2005) in which all external forcings are consistent with observations and future runs (2006-
114 2100) using the RCP8.5 emission scenarios (Taylor et al., 2012). The comparison with the satellite
115 data is made over 2001-2016. To make this comparison, we merged historical runs 2001-2005
116 with RCP8.5 2006-2016.

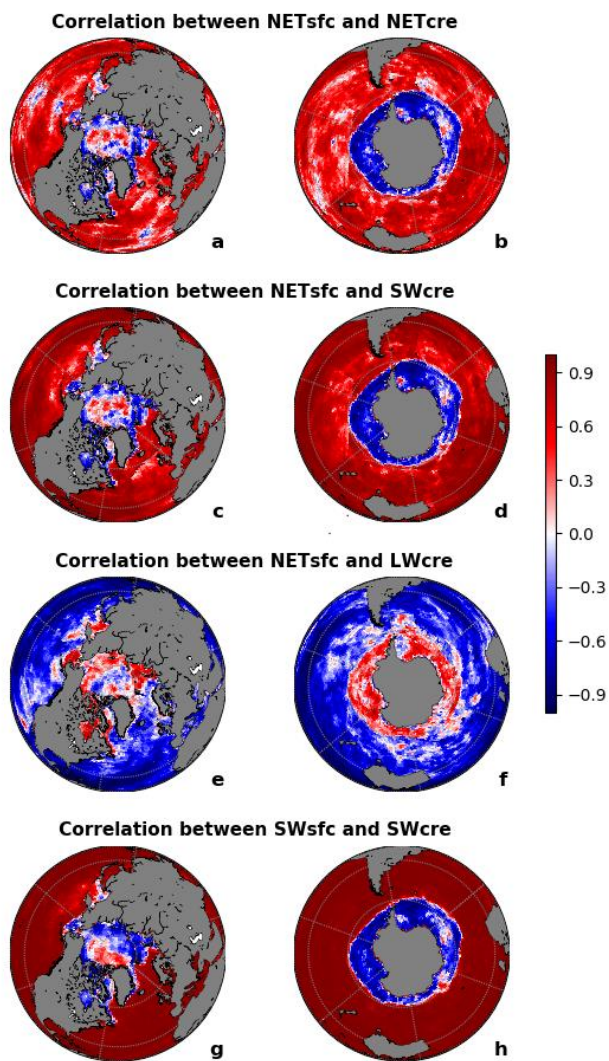
117

118 **3. Results and discussions**

119 **3.1 Negative correlation patterns between cloud radiative effect and surface radiation on** 120 **polar seas**

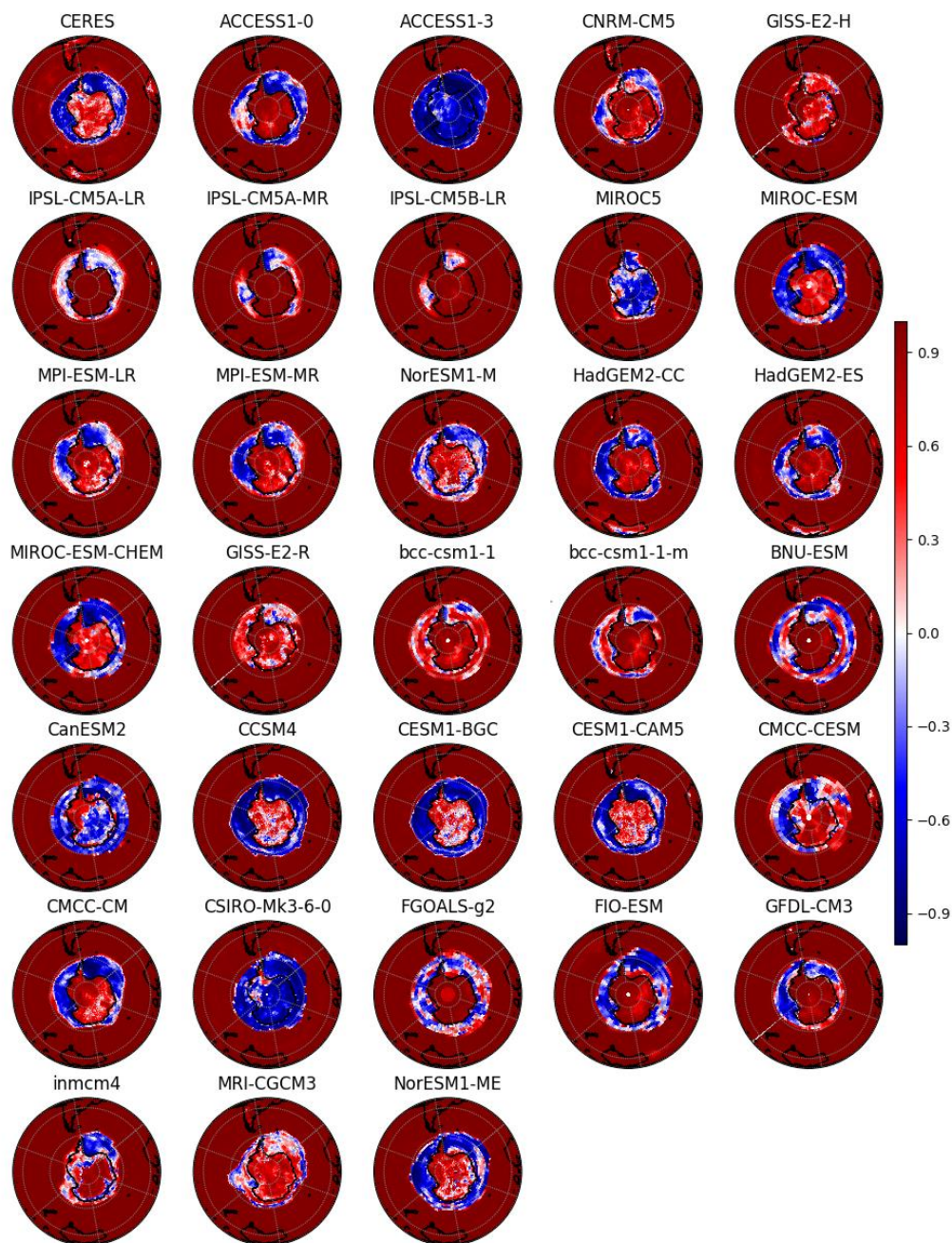
121

122 Given the known cloud influence on the surface radiative budget, a positive correlation between
123 TOA CRE and surface radiative budget is expected (the amount of absorbed radiation at the surface
124 decreases with a more negative SWcre and a less positive LWcre). We find a positive correlation
125 between the net annual CRE ($NET_{cre}=SW_{cre}+LW_{cre}$) and net annual surface radiative flux
126 ($NET_{sfc}=SW_{sfc}+LW_{sfc}$) over much of the global ocean between using the CERES TOA flux data
127 from 2001-2016. However, our analysis reveals the opposite pattern over the polar seas (defined
128 in section 2.5) where the correlation is negative over the Antarctic and partly negative over the
129 Arctic (Bering Strait, Hudson Bay, Barents Sea and the Canadian Archipelago; Fig. 2ab). We split
130 the NET_{cre} into SW_{cre} and LW_{cre} and explore their correlation with the NET_{sfc} . We find that
131 the SW_{cre} (Fig. 2cd) shows similar patterns of correlation as before (Fig. 2ab) but with a stronger
132 magnitude, while LW_{cre} generally shows the opposite correlations (Fig. 2ef). This suggests that
133 SW radiation fluxes are responsible for the sharp contrast between the polar regions and the rest
134 of the world. Indeed, SW_{sfc} and SW_{cre} (Fig. 2gh) show the sharpest and most significant contrast
135 between the polar regions and the rest of the world (Fig. S2 is similar to Fig. 2 but only significant
136 correlations at 95 confidence level are reported in blue and red colors). On average, climate models
137 are able to reproduce the spatial pattern of the observed SW correlation, but show a large inter-
138 model spread concerning the spatial extent of the phenomena (Fig. 3 and S3). On the other hand,
139 several models completely fail at reproducing this fundamental correlation. Indeed, ACCESS1-3,
140 MIROC5, CanESM2 and CSIRO-Mk3-6-0 models shows negative correlation over Antarctic
141 continent in contrast to observed positive correlation. Also, some models like IPSL-CM5B-LR,
142 GISS-E2-R and bcc-csm1-1 completely fail to reproduce the observed negative correlation over
143 the Southern Ocean. This suggests that these models contain misrepresentations of the
144 relationships between sea ice extent, cloud cover/thickness, and/or their influence on surface
145 radiative fluxes that could severely impact their projections.



146

147 **Figure 2** Correlation between TOA CRE and surface radiation over 2001-2016 from CERES
148 measurements for the Northern Hemisphere (aceg) and Southern Hemisphere (bdfh) sea. Positive
149 correlations (red color) indicate that years with less NETsfc coincide with years NETcre has a
150 stronger cooling effect and *vice versa*.



151

152 **Figure 3** Correlation between SWcre and SWsfc shown by 32 CMIP5 earth system models and
153 CERES between 2001 and 2016 over the Southern Hemisphere.



154 3.2 Effects of sea ice concentration change

155

156 We illustrate that the apparent paradox between NET_{cre} and NET_{sfc} found in Fig 2ab is caused
157 by the factors contributing to the SW fluxes. This can be explained by: (I) On the one hand, if
158 cloud properties stay constant and the sea ice (albedo) decreases, SW_{cre} will become increasingly
159 negative (cooling) while more of the incoming shortwave that reaches the surface will be absorbed
160 (warming); (II) On the other hand, the relationship between cloud cover/thickness and sea ice could
161 lead to cloudier Polar seas under melting sea ice (Abe et al., 2016; Liu et al., 2012) such that the
162 SW_{cre} cooling effect is enhanced concurrently with melting sea ice.

163

164 Over the Antarctic seas, analysis of the year-to-year changes in surface downward SW radiation
165 (SW_{down}) stratified in 2% SIC bins retrieved from satellite microwave radiometer measurements
166 shows an increase in SW_{down} with increased SIC and *vice-versa* (Fig. 4a). This suggests that
167 years with higher SIC have fewer and/or thinner clouds (Liu et al., 2012) (Fig. 5), larger SW_{down},
168 and also larger upward SW radiation (SW_{up}) (Fig. 4b), due to the high sea ice albedo (Fig. S4).
169 As a consequence, these years also show a lower SW_{sfc} (Fig. 4c) and thus are characterized by
170 surface cooling. Furthermore, fewer clouds implies a reduction of the cloud cooling effect (less
171 negative SW_{cre}) as described above in process (II), this accounts for $34\% \pm 1\%$ of the total change
172 in SW_{cre}, and as described in process (I) the increase in the surface albedo also makes SW_{cre} less
173 negative and explains $66\% \pm 2\%$ of the observed change (Supplementary section 1 and Fig. 6). This
174 explains the observed negative correlation between SW_{cre} and SW_{sfc} over polar seas and the
175 opposite observed change of SW_{cre} and SW_{sfc} (Fig 4cde). Similar results are found over the
176 Arctic Ocean with slightly different sensitivity (Fig. S5, S6). This difference is tied to differences
177 in sun angle/available sunlight, as Antarctic sea ice is concentrated at lower latitudes than Arctic
178 sea ice.

179

180 Using the regression relationships derived from our composite analysis we can estimate the
181 magnitude of the cloud effect. For the Antarctic system, we use the numbers found in Figure 4e
182 where we find at the annual level, the relationship between NET_{sfc} and SIC, and NET_{cre} and SIC.

183 $\Delta\text{NET}_{\text{sfc}} = (-36.61 \pm 0.72) \Delta\text{SIC}$ (1)

184 $\Delta\text{NET}_{\text{cre}} = (47.03 \pm 1.01) \Delta\text{SIC}$ (2)

185

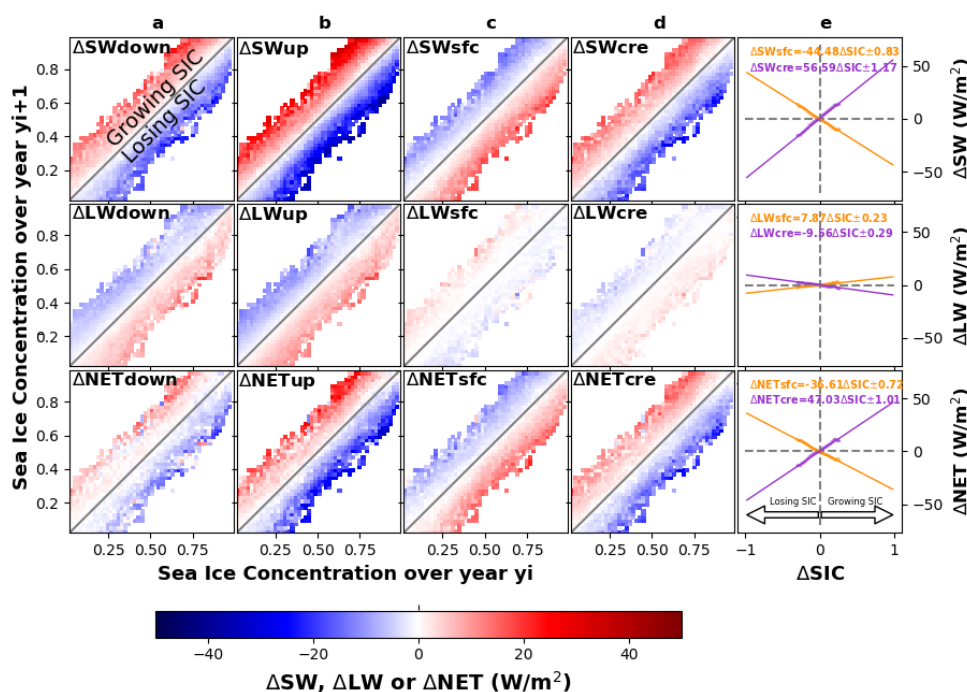
186 In case of excluding the CRE, the $\Delta\text{NET}_{\text{sfc}}$ would be equal to $(-36.61 - 47.03) \Delta\text{SIC} = -83.64 \Delta\text{SIC}$.

187 We estimate that the cloud changes in the Antarctic system are damping by $47.03/83.64 = 56\%$ the
188 potential increase in the surface radiative flux (NET_{sfc}) due to sea ice melting on the surface
189 radiative budget through the surface albedo decrease. The uncertainties of that number are
190 calculated by summing the uncertainties shown in equation (1) and (2) as follows:
191 $(0.72 + 1.01)/83.64 = 2\%$.

192 Similarly, over the Arctic (Fig. S5), we estimate the cloud influence on the surface net radiative
193 budget that covaries with sea ice loss is $47 \pm 3\%$.

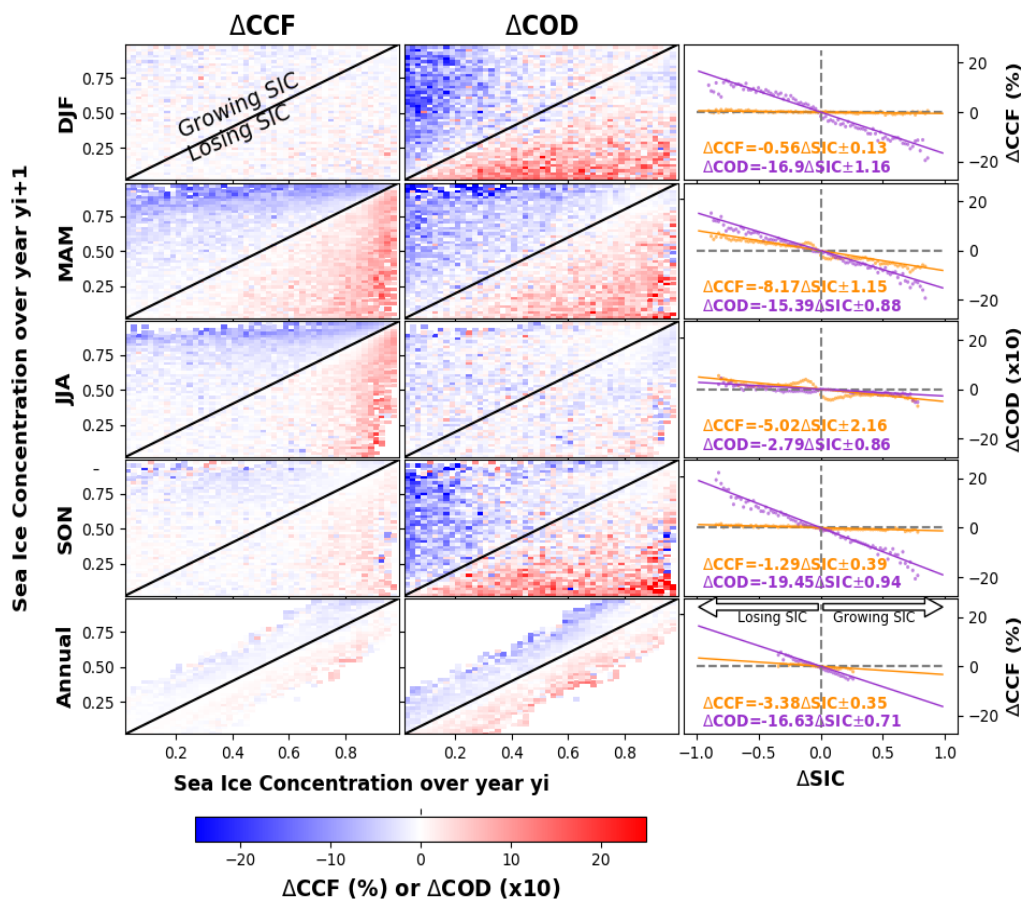


194

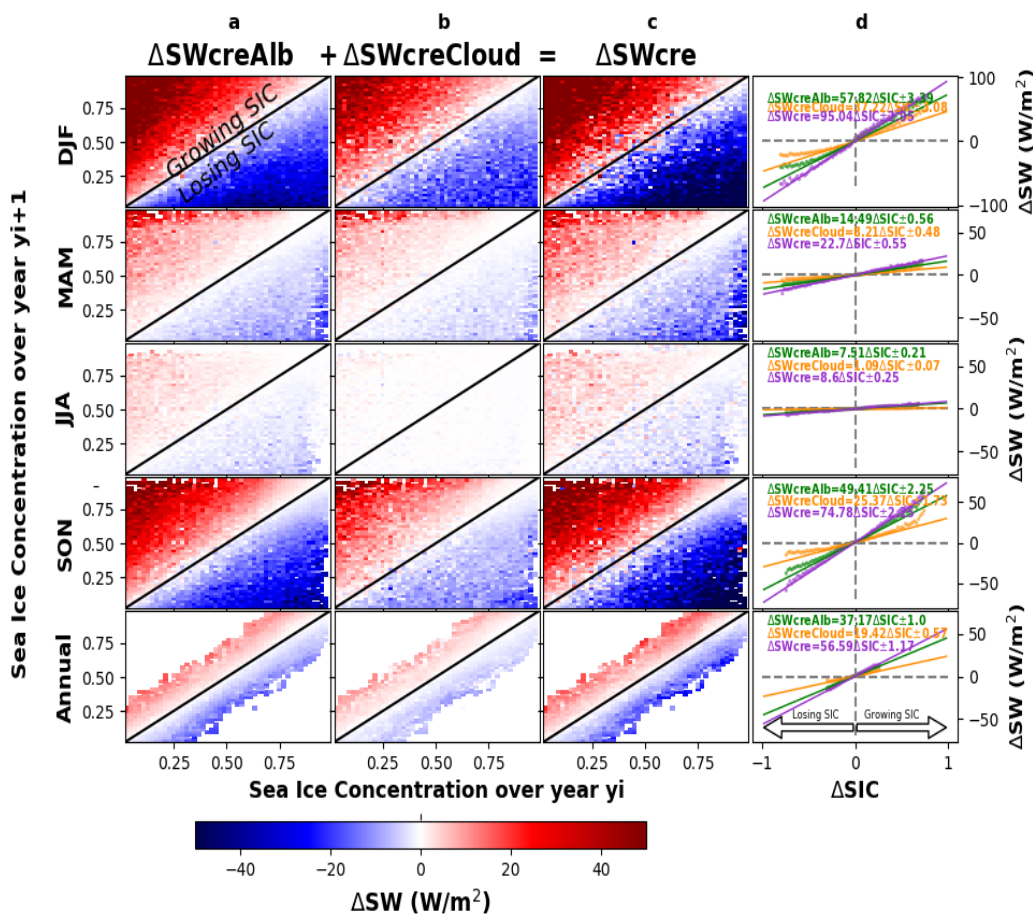


195
 196
 197
 198
 199
 200
 201
 202
 203
 204

Figure 4 Annual changes in SW, LW and NET as function of SIC. Annual changes in SW (top), LW (middle) and NET (bottom) of radiative down (a), up (b), sfc=down-up (c) and cre (d) over Antarctic sea as function of SIC change between two consecutive years y_{i+1} and y_i from 2001–2016 time period. The top triangles in (c top) refers to the increase (growing) in SIC while the blue color means a reduction (cooling) in SW_{sfc} . Whereas, the top triangles in (d) refers to the increase in SIC while the red color means an increase (decreasing the cooling role of clouds) in SW_{cre} . Each dot in column (e) represents the average of one parallel to the diagonal in (c) or (d) as described in the Supplement section 2.



205
 206 **Figure 5** Seasonal and annual changes in cloud cover fraction (CCF) and cloud optical depth
 207 (COD) over the Antarctic polar sea region as a function of SIC change between two consecutive
 208 years y_{i+1} and y_i from 2001-2016 time period. In order to use the same scale, COD has been
 209 multiplied by a factor 10. The top triangles in the two first columns refers to the increase (growing)
 210 in SIC while the blue color means a reduction in CCF or COD.
 211



212

213 **Figure 6** Seasonal and annual changes in SWcreAlb, SWcreCloud and SWcre over the Antarctic
 214 polar sea region as function of SIC change between two consecutive years y_{i+1} and y_i from 2001-
 215 2016 time period. The analysis is based on observations from satellites data.

216

217

218

219

220

221

222



223 Altogether these results suggesting that polar sea ice and cloud covarying in a way that
224 substantially reduces the overall impact of the sea ice loss. In fact, with melting of the sea ice the
225 cooling effects of clouds are enhanced. This effect in the polar climate system leads to a substantial
226 reduction ($56\pm 3\%$ over the Antarctic and $47\pm 3\%$ over the Arctic) of the potential increase in
227 NETsfc in response to sea ice loss. Despite this mechanism, the sharp reduction in Arctic surface
228 albedo has been dominating the recent change in the surface radiative budget and led to a
229 significant increase in NETsfc since 2001. These results demonstrate that the interannual
230 variability of polar surface radiative fluxes is currently controlled by variations in SIC and surface
231 albedo, and that cloud effects only mitigate the effects but not invert the trends (i.e., a damping
232 effect). Our findings highlight the importance of processes that control sea ice albedo (i.e. sea ice
233 dynamics, snowfall, melt pond formation, and the deposition of black carbon), as the surface
234 albedo of the polar seas in regions of seasonal sea ice is crucial for the climate dynamics.

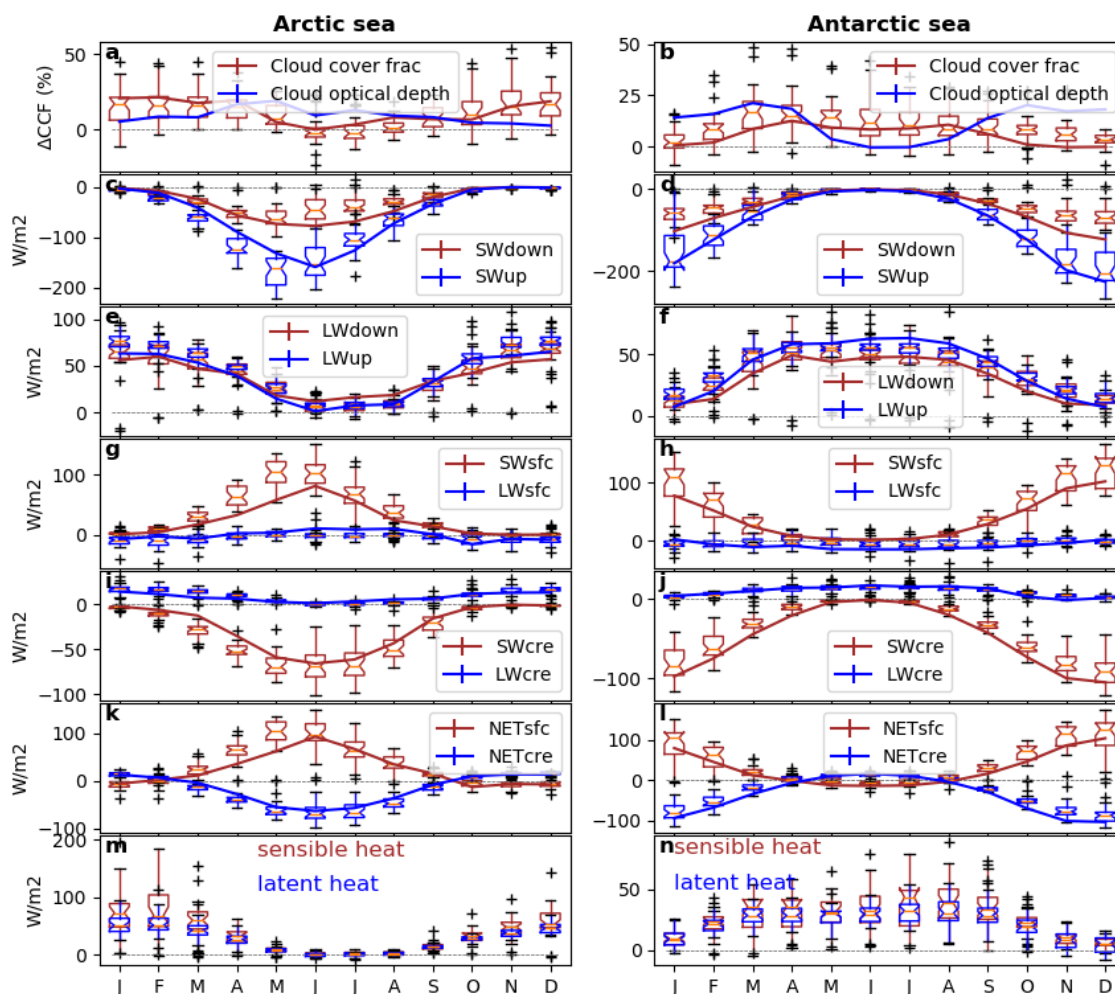
235 **3.3 Sensitivity of the surface energy budget to variability of sea ice concentration**

236 Our results are consistent with other recent studies (Taylor et al., 2015) that demonstrate a cloud
237 cover fraction (CCF) response to reduced sea ice in fall/winter but not in summer (Figure 7a) over
238 the Arctic Ocean. The lack of a summer time cloud response to sea ice loss is explained by the
239 prevailing air-sea temperature gradient in summer, where near surface air temperatures are
240 frequently warmer than the surface temperature. Surface temperatures in regions of sea ice melting
241 hover near freezing due to the phase change, whereas the atmospheric temperatures are not
242 constrained by the freezing/melting point. Despite reduced sea ice cover, strong increases in
243 surface evaporation (latent heat) are limited (Fig. 7mn), as also suggested by the small trends in
244 surface evaporation rate derived from satellite-based estimates (Boisvert and Stroeve, 2015; Taylor
245 et al., 2018). We argue that the strong increase of SWcre under decreased sea ice observed during
246 summer is induced by larger values of cloud optical depth (Fig. 7a), which depends directly on the
247 liquid or ice water content. We also show that the relationships derived from our observation-
248 driven analysis match the projected changes in the Arctic and Antarctic surface energy budget in
249 the median CMIP5 model ensemble (Fig. 7). However, the large spread amongst climate models
250 indicates that there is still considerable uncertainty.

251 Analyzing the seasonal cycle of the sensitivity of the surface energy budget to SIC variability, we
252 found that SWsfc (SWcre) explains most of the observed changes in the NETsfc (NETcre) during
253 summer, while LWsfc plays a minor role (Fig. 7). In contrast, during winter LWsfc (LWcre)
254 explains most of the observed changes in the NETsfc (NETcre). In general, the median of the 32
255 CMIP5 (Taylor et al., 2012) climate models captures the observed sensitivity of the radiative
256 energy budget and cloud cover change to SIC but the spread between climate models is large,
257 especially for cloud cover fraction. We have to note here that, the numbers reported in Figure 7
258 are for 100% SIC loss, while the ones reported in the previous figures (Fig. 4, 5 and 6) are for
259 100% SIC gain and explains the opposite sign.

260

261



262
 263 **Figure 7** Monthly change in different terms of the radiative energy balance, cloud optical depth
 264 (COD) and cloud cover fraction (CCF) extrapolated from observation for an hypothetical 100%
 265 decrease in SIC over the areas where we observed SIC change during the period 2001-2016. This
 266 change estimate came from the use of a linear interpolation of the change of different parts of
 267 energy balance, COD and CCF as function of change in SIC coming from all possible
 268 combinations of couples of consecutive years for a given month from 2001 to 2016 and for all grid
 269 cells for which SIC is larger than zero in one of the two years. Observations are shown by solid
 270 lines (the standard deviation of the slopes are also reported but are too small to be visible) while
 271 CMIP5 models are shown by boxplot and the box (are in same color as observations) represents
 272 the first and third quartiles (whiskers indicate the 99% confidence interval and black markers show
 273 outliers). In order to use the same scale, COD has been multiplied by a factor 10.

274
 275



276 3.4 Projections and uncertainties of cloud radiative effects on surface energy budget

277 In the future, under RCP8.5 scenario (a business as usual case) (Taylor et al., 2012), CMIP5 models
278 show an increase in SWsfc over the Arctic Ocean (Fig. 8a) coherent with the expected large
279 decrease in the SIC (Comiso et al., 2008; Serreze et al., 2007; Stroeve et al., 2007). This increase
280 in SWsfc happens despite the relatively large, concurrent and opposing change in cloud cooling
281 effect (SWcre). Future fluxes of LW (Fig. 8c) will likely play a minor but non-negligible role on
282 total energy budget by further increasing the surface net radiative fluxes, NETsfc (Fig. 8e),
283 damping the cooling effect of clouds NETcre. In addition, CMIP5 models shows clearly that by
284 2100, the magnitude of the decrease in NETcre is slightly lower than the increase in NETsfc (Fig.
285 8e) over Arctic Ocean. While the Antarctic polar sea region shows the opposite (Fig. 8f). This is
286 in line with the estimated dampening effect of clouds coming from CERES over 2001-2016 that
287 is about $47\pm 3\%$ in the Arctic and $56\pm 2\%$ in the Antarctic.

288

289 Large uncertainties remain on the decline rate of summer sea ice and the timing of the first
290 occurrence of a sea ice-free Arctic summer (Arzel et al., 2006; Zhang and Walsh, 2006). The
291 reason behind the large spread between climate models is still debated (Holland et al., 2017;
292 Simmonds, 2015; Turner et al., 2013). In this study, we explored the mean annual Arctic and
293 Antarctic sea-ice extent trend coming from 32 CMIP5 models and find a high positive correlation
294 with the simulated trend in the SWdown (Figure 8gh). This analysis suggests that the models
295 showing a larger trend in cloud cover also show larger decreases in sea-ice extent and clearly
296 demonstrate the strong coupling of these two variables.

297

298 4. Conclusion

299 The manuscript deals with two important and controversial topics in climate science, namely the
300 role of clouds and the fate of polar sea ice. The work is grounded in a long time series of robust
301 satellite observations that allowed us to document an important damping effect in the polar clouds-
302 sea ice system. In addition, we show how 32 state-of-the-art climate models represent this
303 feedback.

304

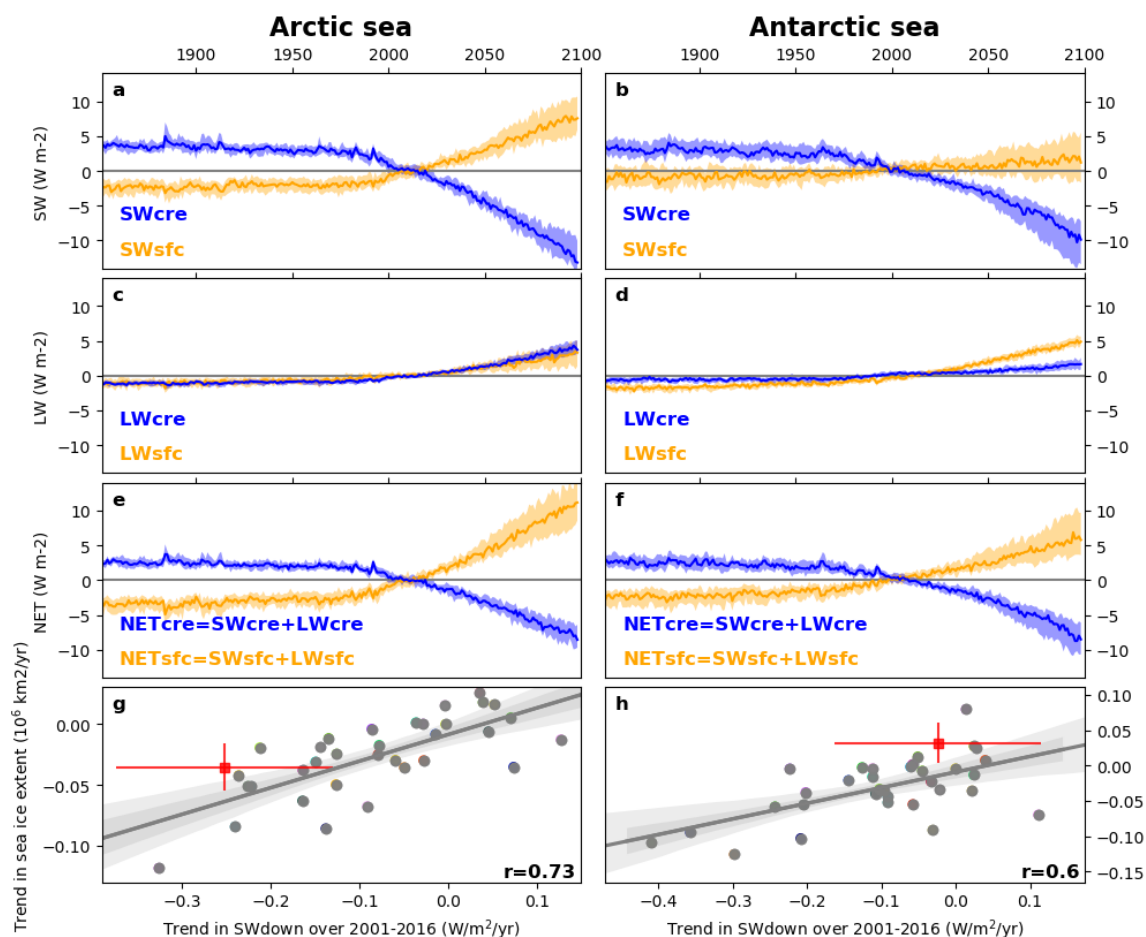
305 Our data-driven analysis shows that polar sea-ice and clouds interplay in a way that substantially
306 reduces the overall impact of the sea ice loss. We found that when sea ice cover is reduced between
307 two consecutive years that the cooling effect of clouds increased, damping the total change in the
308 net surface energy budget. The magnitude of this effect is important. Satellite data indicates that
309 the increased cloud cover/thickness correlates with sea ice melting, reducing by half the potential
310 increase of net radiation at the surface. One-third of this half is induced by the direct change in
311 cloud cover/thickness. While 2/3rd of this effect is the result of changing surface albedo. This
312 finding challenges the classic view that minimizes the relationship between summer clouds and
313 sea ice concentration (Taylor et al., 2015), and demonstrates that less sea ice, even during summer,
314 leads to thicker clouds that reduces the fraction of solar energy reaching the surface.



315 In addition, we demonstrated that the models that shows larger trends in polar sea ice extent are
316 the same that show smaller trends in surface incoming solar radiation (clouds). In order to
317 understand current and future climate trajectories, model developments should aim to reduce
318 uncertainties in the representation of polar cloud processes and their relationships with sea ice
319 cover. The observation-driven findings reported in the manuscript could be instrumental for this
320 scope.

321

322 Future cloud changes and sea evolution represent major uncertainties in climate projections due to
323 the multiple and relevant pathways through which cloudiness and sea ice feed back on the Earth's
324 climate system (Solomon, S., D. Qin, M. Manning, Z. Chen, M. Marquis, K.B. Averyt, 2007). Our
325 evidence derived from Earth observations may substantially reduce the uncertainty on the
326 covariation between polar clouds and the changing sea ice cover (Fig. 7), constrain future model
327 projections and ultimately improve the understanding of present and future polar climate.
328 Ultimately, our findings on the interplay between cloud and sea ice may support an improvement
329 in the model representation of the cloud-ice feedback, a mechanism that may affect the speed of
330 the polar sea ice retreat, which in turn has a broad impact on the climate system, on the Arctic
331 environment and on potential economic activities in Arctic regions (Buixadé Farré et al., 2014).



332

333 **Figure 8** Time series of the anomaly of the radiative flux over the period 1850-2100. Mean
 334 modeled SWcre, LWcre and NETcre (blue) and surface SWsfc, LWsfc and NETsfc (orange)
 335 anomalies over the 1850-2100 period under rcp8.5 scenario averaged over the Arctic sea. The solid
 336 line shows the median, where the envelope represents the 25 and 75 percentile of the 32 CMIP5
 337 models. The linear regression (grey solid line and its 68% (dark grey envelope) and 95% (light
 338 grey envelope) confidence interval) between: the trend in SWdown and trend in sea ice extent (g
 339 and h); of the 32 CMIP5 climate models shown by grey dots over 2001-2016. The observed trends
 340 are shown by red colors where confidence interval refers to standard error of the trend.

341

342

343

344



345 **Acknowledgments:** The authors acknowledge the use of Clouds and the Earth's Radiant Energy
346 System (CERES) satellite data version 4.0 from <https://ceres.larc.nasa.gov/index.php>, sea ice
347 concentration data from National Snow and Ice Data Center (NSIDC) <http://nsidc.org/data/G02202>, as
348 well as the modeling groups that contributed to the CMIP5 data archive at PCMDI
349 <https://cmip.llnl.gov/cmip5/>.

350

351 **Author Contributions:** RA designed the study and performed the analysis. RA, AC, PCT and LGS
352 contributed to the interpretation of the results. RA, PCT, AC and GD drafted the paper. All authors
353 commented on the text.

354 **Competing interests:** The authors declare no competing financial interests.

355 **Additional information:** The programs used to generate all the results are made with Python.
356 Analysis scripts are available by request to R. Alkama.

357 **References:**

358

359 Abe, M., Nozawa, T., Ogura, T. and Takata, K.: Effect of retreating sea ice on Arctic cloud cover
360 in simulated recent global warming, *Atmos. Chem. Phys.*, 16, 14343–14356, doi:10.5194/acp-16-
361 14343-2016, 2016.

362

363 Arzel, O., Fichefet, T. and Goosse, H.: Sea ice evolution over the 20th and 21st centuries as
364 simulated by current AOGCMs, *Ocean Model.*, 12(3-4), 401–415,
365 doi:10.1016/J.OCEMOD.2005.08.002, 2006.

366

367 Boisvert, L. N. and Stroeve, J. C.: The Arctic is becoming warmer and wetter as revealed by the
368 Atmospheric Infrared Sounder, *Geophys. Res. Lett.*, 42(11), 4439–4446,
369 doi:10.1002/2015GL063775, 2015.

370

371 Buixadé Farré, A., Stephenson, S. R., Chen, L., Czub, M., Dai, Y., Demchev, D., Efimov, Y.,
372 Graczyk, P., Grythe, H., Keil, K., Kivekäs, N., Kumar, N., Liu, N., Matelenok, I., Myksovoll, M.,
373 O’Leary, D., Olsen, J., Pavithran.A.P., S., Petersen, E., Raspotnik, A., Ryzhov, I., Solski, J., Suo,
374 L., Troein, C., Valeeva, V., van Rijckevorsel, J. and Wighting, J.: Commercial Arctic shipping
375 through the Northeast Passage: routes, resources, governance, technology, and infrastructure,
376 *Polar Geogr.*, 37(4), 298–324, doi:10.1080/1088937X.2014.965769, 2014.

377

378 Charlock, T. P. and Ramanathan, V.: The Albedo Field and Cloud Radiative Forcing Produced
379 by a General Circulation Model with Internally Generated Cloud Optics, *J. Atmos. Sci.*, 42(13),
380 1408–1429, doi:10.1175/1520-0469(1985)042<1408:TAFACR>2.0.CO;2, 1985.

381

382 Cheung, W. W. L., Lam, V. W. Y., Sarmiento, J. L., Kearney, K., Watson, R. and Pauly, D.:
383 Projecting global marine biodiversity impacts under climate change scenarios, *Fish Fish.*, 10(3),
384 235–251, doi:10.1111/j.1467-2979.2008.00315.x, 2009.

385



- 386 Cohen, J., Screen, J. A., Furtado, J. C., Barlow, M., Whittleston, D., Coumou, D., Francis, J.,
387 Dethloff, K., Entekhabi, D., Overland, J. and Jones, J.: Recent Arctic amplification and extreme
388 mid-latitude weather, *Nat. Geosci.*, 7(9), 627–637, doi:10.1038/ngeo2234, 2014.
389
- 390 Comiso, J. C., Comiso, J. C., Parkinson, C. L., Gersten, R., Stock, L., Parkinson, C. L., Gersten,
391 R. and Stock, L.: Accelerated decline in the arctic sea ice cover, *Geophys. Res. Lett.* [online]
392 Available from: <http://citeseerx.ist.psu.edu/viewdoc/summary?doi=10.1.1.419.8464> (Accessed
393 30 March 2018), 2008.
394
- 395 Graverson, R. G., Mauritsen, T., Tjernström, M., Källén, E. and Svensson, G.: Vertical structure
396 of recent Arctic warming, *Nature*, 451(7174), 53–56, doi:10.1038/nature06502, 2008.
397
- 398 Harrison, E. F., Minnis, P., Barkstrom, B. R., Ramanathan, V., Cess, R. D. and Gibson, G. G.:
399 Seasonal variation of cloud radiative forcing derived from the Earth Radiation Budget
400 Experiment, *J. Geophys. Res.*, 95(D11), 18687, doi:10.1029/JD095iD11p18687, 1990.
401
- 402 Holland, M. M., Landrum, L., Raphael, M. and Stammerjohn, S.: Springtime winds drive Ross
403 Sea ice variability and change in the following autumn, *Nat. Commun.*, 8(1), 731,
404 doi:10.1038/s41467-017-00820-0, 2017.
405
- 406 Kato, E., Kinoshita, T., Ito, A., Kawamiya, M. and Yamagata, Y.: Evaluation of spatially explicit
407 emission scenario of land-use change and biomass burning using a process-based
408 biogeochemical model, *J. Land Use Sci.*, 8(1), 104–122, doi:10.1080/1747423X.2011.628705,
409 2013.
410
- 411 Liu, Y., Key, J. R., Liu, Z., Wang, X. and Vavrus, S. J.: A cloudier Arctic expected with
412 diminishing sea ice, *Geophys. Res. Lett.*, 39(5), n/a–n/a, doi:10.1029/2012GL051251, 2012.
413
- 414 Loeb, N. G., Doelling, D. R., Wang, H., Su, W., Nguyen, C., Corbett, J. G., Liang, L., Mitrescu,
415 C., Rose, F. G., Kato, S., Loeb, N. G., Doelling, D. R., Wang, H., Su, W., Nguyen, C., Corbett, J.
416 G., Liang, L., Mitrescu, C., Rose, F. G. and Kato, S.: Clouds and the Earth’s Radiant Energy
417 System (CERES) Energy Balanced and Filled (EBAF) Top-of-Atmosphere (TOA) Edition-4.0
418 Data Product, *J. Clim.*, 31(2), 895–918, doi:10.1175/JCLI-D-17-0208.1, 2018.
419
- 420 Peng, G., Meier, W. N., Scott, D. J. and Savoie, M. H.: A long-term and reproducible passive
421 microwave sea ice concentration data record for climate studies and monitoring, *Earth Syst. Sci.*
422 *Data*, 5(2), 311–318, doi:10.5194/essd-5-311-2013, 2013.
423
- 424 Post, E., Bhatt, U. S., Bitz, C. M., Brodie, J. F., Fulton, T. L., Hebblewhite, M., Kerby, J., Kutz,
425 S. J., Stirling, I. and Walker, D. A.: Ecological consequences of sea-ice decline., *Science*,
426 341(6145), 519–24, doi:10.1126/science.1235225, 2013.
427
- 428 Ramanathan, V., Cess, R. D., Harrison, E. F., Minnis, P., Barkstrom, B. R., Ahmad, E. and
429 Hartmann, D.: Cloud-radiative forcing and climate: results from the Earth radiation budget
430 experiment., *Science* (80-.), 243(4887), 57–63, doi:10.1126/science.243.4887.57, 1989.
431



- 432 Serreze, M. C., Holland, M. M. and Stroeve, J.: Perspectives on the Arctic's Shrinking Sea-Ice
433 Cover, *Science* (80-.), 315(5818), 1533–1536, doi:10.1126/science.1139426, 2007.
434
- 435 Simmonds, I.: Comparing and contrasting the behaviour of Arctic and Antarctic sea ice over the
436 35 year period 1979-2013, *Ann. Glaciol.*, 56(69), 18–28, doi:10.3189/2015AoG69A909, 2015.
437
- 438 Solomon, S., D. Qin, M. Manning, Z. Chen, M. Marquis, K.B. Averyt, M. T. and H. L. M.:
439 Contribution of Working Group I to the Fourth Assessment Report of the Intergovernmental
440 Panel on Climate Change, 2007. [online] Available from:
441 http://www.ipcc.ch/publications_and_data/ar4/wg1/en/contents.html (Accessed 2 July 2018),
442 2007.
443
- 444 Stroeve, J., Holland, M. M., Meier, W., Scambos, T. and Serreze, M.: Arctic sea ice decline:
445 Faster than forecast, *Geophys. Res. Lett.*, 34(9), doi:10.1029/2007GL029703, 2007.
446
- 447 Taylor, K. E., Stouffer, R. J. and Meehl, G. A.: An Overview of CMIP5 and the Experiment
448 Design, *Bull. Am. Meteorol. Soc.*, 93(4), 485–498, doi:10.1175/BAMS-D-11-00094.1, 2012.
449
- 450 Taylor, P., Hegyi, B., Boeke, R. and Boisvert, L.: On the Increasing Importance of Air-Sea
451 Exchanges in a Thawing Arctic: A Review, *Atmosphere (Basel)*, 9(2), 41,
452 doi:10.3390/atmos9020041, 2018.
453
- 454 Taylor, P. C., Kato, S., Xu, K.-M. and Cai, M.: Covariance between Arctic sea ice and clouds
455 within atmospheric state regimes at the satellite footprint level, *J. Geophys. Res. Atmos.*,
456 120(24), 12656–12678, doi:10.1002/2015JD023520, 2015.
457
- 458 Turner, J., Bracegirdle, T. J., Phillips, T., Marshall, G. J., Hosking, J. S., Turner, J., Bracegirdle,
459 T. J., Phillips, T., Marshall, G. J. and Hosking, J. S.: An Initial Assessment of Antarctic Sea Ice
460 Extent in the CMIP5 Models, *J. Clim.*, 26(5), 1473–1484, doi:10.1175/JCLI-D-12-00068.1,
461 2013.
462
- 463 W. Meier, F. Fetterer, M. Savoie, S. Mallory, R. Duerr, and J. S.: NOAA/NSIDC Climate Data
464 Record of Passive Microwave Sea Ice Concentration, Version 3. Boulder, Colorado USA.
465 NSIDC: National Snow and Ice Data Center., , doi:<https://doi.org/10.7265/N59P2ZTG>, 2017.
466
- 467 Zhang, X. and Walsh, J. E.: Toward a Seasonally Ice-Covered Arctic Ocean: Scenarios from the
468 IPCC AR4 Model Simulations, *J. Clim.*, 19(9), 1730–1747, doi:10.1175/JCLI3767.1, 2006.
469
470